THE ASTROPHYSICAL JOURNAL, 379:295–309, 1991 September 20

SEARCHES FOR MILLISECOND PULSATIONS IN LOW-MASS X-RAY BINARIES

K. S. WOOD, J. P. NORRIS,[1] AND P. HERTZ
Code 4121, E. O. Hulburt Center for Space Research, Naval Research Laboratory, Washington, DC 20375
B. A. VAUGHAN AND P. F. MICHELSON
Department of Physics, Stanford University, Stanford, CA 94305
K. MITSUDA
Institute for Space and Astronautical Science, 3-1-1 Yoshinodai, Sagamihara, Kanagawa 229, Japan
W. H. G. LEWIN
Room 37-627, Center for Space Research and Department of Physics, Massachusetts Institute of Technology, Cambridge, MA 02139
AND
J. VAN PARADIJS, W. PENNINX,[2] AND M. VAN DER KLIS
Astronomical Institute "Anton Pannekoek," University of Amsterdam, Roettersstraat 15, 1018 WB Amsterdam, The Netherlands, and Center for High-Energy Astrophysics, Amsterdam
Received 1990 August 6; accepted 1991 February 13

ABSTRACT

Recent observational and theoretical studies of low-mass X-ray binaries (LMXBs) have given rise to a new class of standard models. In these models, accretion torques have spun the neutron star primary up to millisecond rotation periods. The existence of both millisecond radio pulsars and quasi-periodic X-ray oscillations is interpreted as supporting millisecond spin periods. However, millisecond spin periods remain undetected in low-mass X-ray binaries.

Detection of the low pulse fractions expected for binary millisecond X-ray pulsars requires long integration times to enhance signal to noise. One of the significant barriers to detection is the pulse phase modulation which occurs when signals are integrated over a significant portion of a binary orbital cycle. We derive an optimized one-parameter Coherence Recovery Technique (CRT) for recovery of phase coherence. This technique affords a large increase in sensitivity over the method of incoherent summation of Fourier power spectra. In CRT a sequence of quadratic time transformations is applied to the data, followed by a Fourier transform for each trial. One particular transformation results in maximal compensation for the phase modulation and minimization of frequency broadening in the power spectrum. We discuss the range of spin periods expected from LMXB phenomenology, describe necessary constraints on the application of CRT in terms of integration time and orbital parameters, and estimate the residual power unrecovered by the quadratic approximation for realistic cases. An alternative, equivalent CRT approach is described in which a single Fourier transform of the data is followed by the application of a Wiener filter matrix in frequency space.

We have applied CRT to high time resolution observations (0.3–5 ms) of several LMXBs obtained with the *Ginga* and *HEAO 1* X-ray satellites. We present upper limits on the pulsed fluxes from Sco X-1, GX 340+0, GX 5−1, GX 9+1, GX 17+2, 4U 1820−30, Cyg X-3, and Cyg X-2. The 95% confidence level upper limit to the pulse fraction for sinusoidal pulses from the two brightest sources observed, Sco X-1 and GX 5−1, is less than 0.7% for frequencies up to 512 Hz, and less than 0.4% for frequencies less than 100 Hz. Our study implies that pulsars in LMXBs must have low pulse fractions ($A < 1\%$), have short pulse periods ($P_{\rm pul} < 2$ ms), or, in those cases where the orbital periods are unknown, be in binary orbits with short orbital periods ($P_{\rm orb} < 3$ hr)

Subject headings: numerical methods — stars: neutron — pulsars — X-rays: binaries

1. INTRODUCTION

In a majority of the Galactic X-ray binary systems containing neutron stars, the spin period of the neutron star is currently unknown. In the subclass of low-mass X-ray binaries (LMXBs), the dearth of known spin periods is especially striking, there being almost no measured spin periods. The standard picture of a LMXB system comprises a neutron star with magnetic field of order 10^9 G accreting 10^{-10}–10^{-8} $M_\odot$ yr^{-1} of material from a low-mass companion that is probably a late-type dwarf (Lewin & Joss 1983; Lewin, van Paradijs, & van der Klis 1988). Two LMXBs for which the spin periods are known, 4U 1626−67 (7.6 s) and 1H 2259+586 (7.0 s), are anomalous, showing evidence of different evolutionary histories from other LMXBs. Her X-1 and GX 1+4, which also have known spin periods and whose companions' masses fall within the mass range for LMXBs, have magnetic fields of roughly 10^{12} G. Apart from these four, no other spin periods are known in the class of LMXBs.

The roughly two dozen known binary pulsars belong almost entirely to the high-mass X-ray binary (HMXB) class, which accounts for fewer than half the known Galactic neutron star binary systems. Within the HMXB group spin periods range from 0.069 s (A 0538−66) to 13 minutes (X Per). Several non-

[1] Postal address: Code 690, Laboratory for High-Energy Astrophysics, NASA Goddard Space Flight Center, Greenbelt, MD 20771.
[2] Also Center for Space Research and Department of Physics, Massachusetts Institute of Technology.

pulsing sources in the HMXB group are black hole candidates (e.g., Cyg X-1, LMC X-1, LMC X-3). The HMXB group appears to be substantially younger than the LMXB group. Evidence for this includes their relatively higher masses, their location in Population I regions of the Galaxy, and the strong fields of neutron stars in HMXBs. In seeking periods within the LMXBs, HMXB periods are not a reliable guide. Instead, millisecond spin periods are suspected for LMXBs.

The spin period, $P_{\rm spin}$, is arguably the most important parameter to determine in these systems. It is critical for our understanding of the evolution of LMXBs and their connection with millisecond radio pulsars. This paper describes a new, sensitive search for spin periods in several LMXB sources, with emphasis on millisecond periods. Power spectra for these sources typically show a DC level, low- and high-frequency noise, and occasional quasi-periodic oscillations (QPOs), without detectable coherent pulsations at any frequency. In accreting neutron stars $P_{\rm spin}$ is largely a consequence of the mass accretion rate and magnetic moment, that is, it is an integral over the history of the (principally accretion) torques applied to the star. For LMXB systems estimates of spin periods are largely dependent upon assumptions about the torque history. Detection of pulsations due to neutron star spin would make it possible to determine orbital characteristics and source masses to high precision and would lead to the kinds of studies that have been done with binary pulsars, including spin period fluctuation studies, but with greatly improved precision owing to the short period.

In the absence of detected spin periods, much has been established about LMXBs using other evidence. The total luminosity and the detections of X-ray bursts confirm the basic assumption that the accreting object is a neutron star. The theory of X-ray bursts can be used to obtain a ceiling on the magnetic field of about 10^{10} G. The particular variety of quasi-periodic oscillations known as horizontal branch oscillations also require a weak magnetic field, of the order 10^9 G. These magnetic field estimates, combined with a standard disk accretion model, predict LMXB spin periods in the millisecond range. Weak fields help explain the lack of conspicuous pulsations, but do not rule out coherent pulsations at low levels of modulation.

We have designed high-sensitivity search techniques for millisecond periods and applied these methods to data from the Japanese satellite *Ginga* and *HEAO 1*. The search is optimized for pulsed signals whose period, drift rate, and amplitude conform with what is expected for LMXB sources, that is, we search for millisecond pulsations with drift rates of the magnitude inferred from binary orbit characteristics. In § 2 we describe how current understanding of LMXBs guides the search strategy and sets these parameter limits. We derive the optimum search technique, called the *Coherence Recovery Technique*, in § 3. In § 4 we present the observations and in § 5 describe implications of the results.

2. PARAMETER RANGES FOR PULSATION SEARCHES

2.1. *Spin Period Estimates*

Estimates of the expected spin periods in LMXBs are based on angular momentum transfer in postulated accretion environments, possible links between LMXBs and other neutron star populations, and understanding of neutron star behavior at high spin frequencies.

Angular momentum transfer by accretion can be estimated from the mass accretion rate $\dot{M}$, the accretion geometry, and the magnetic moment of the neutron star μ. In the high-luminosity LMXBs the bulk of the mass transfer is assumed to be via a conventional viscous accretion disk (Shakura & Sunyaev 1973). The instantaneous angular momentum transfer rate is a function of $\dot{M}$, μ, and $P_{\rm spin}$, while the equilibrium spin period, $P_{\rm eq}$, is a function of $\dot{M}$ and μ. For the disk accretion torque model of Ghosh & Lamb (1979a, b) the equilibrium value is given by

$$P_{\rm eq} = (3.9\ {\rm ms})\mu_{27}^{6/7} M_{\rm ns}^{-2/7} R_6^{-3/7} L_{38}^{-3/7}\ , \qquad (1)$$

where $M_{\rm ns}$ is the neutron star mass in $M_\odot$, R_6 is the stellar radius in units of 10^6 cm, L_{38} is the X-ray luminosity in units of 10^{38} ergs s^{-1}, and μ_{27} is the magnetic moment in units of 10^{27} G cm^3.

The oldest approach to estimating magnetic moments in LMXBs consists of estimating field evolution from physical models. The simplest picture assumes a universal initial field of 10^{12}–10^{13} G, decaying exponentially with a time constant of about $10^{6.7}$ yr to 10^9 G and 10^9–10^{10} yr afterward (Taam & van den Heuvel 1986). Crude LMXB age estimates then indicate 10^9–10^{10} G fields. This picture is almost surely too simple for LMXBs. Several other factors proposed to enter into the field evolution include possible stable minimum values below which the field cannot decay and other mechanisms for field decay or alignment (Kulkarni 1986; van den Heuvel, van Paradijs, & Taam 1986; Bhattacharya 1989; Shibazaki et al. 1989; Romani 1990). The range of values derived in these models is 10^8–10^{10} G.

Another estimation technique exploits the fact that X-ray bursts occur in some LMXBs (see, e.g., Lewin & Joss 1983). Thermonuclear runaway models yield a critical accretion rate above which bursting is suppressed and only stable nuclear burning occurs. This limit is derived assuming uniform accretion over the stellar surface in a spherically symmetric model, hence it can be taken as a limit on a mass accretion rate per unit area (Joss 1978). If a magnetic field channels flow to a polar cap, then the maximum rate is reduced by the ratio of polar cap area to total stellar surface area. A strong field thus allows bursts to be suppressed at comparatively lower mass accretion rates. Observations confirm the existence of the critical accretion rate; the observed value and the theory require a stellar field less than 10^{10} G (Taam & van den Heuvel 1986).

A third method uses quasi-periodic oscillations found in some LMXBs (see, e.g., Lewin et al. 1988). The beat frequency model (Alpar & Shaham 1985; Lamb et al. 1985) for the horizontal branch QPO mode (HBO) requires neutron stars with magnetic fields $\sim 5 \times 10^9$ G and spin frequencies of ~ 100 Hz. However, recent analyses indicate problems with the beat frequency model (Shibazaki 1989; Norris et al. 1990; Mitsuda et al. 1990).

When magnetic moments in the range of these various estimates (10^{27}–10^{28} G cm^3) are substituted into equation (1), a period in the millisecond range is derived. This is part of the basis for the suggestion of an evolutionary link between LMXB sources and radio millisecond pulsars (Helfand, Ruderman, & Shaham 1983; Joss & Rappaport 1983; Paczynski 1983; Savonije 1983; cf. Ruderman 1990). Using this hypothesis we gain a fourth estimate of magnetic field strength: it should equal or exceed the value now derived for radio millisecond pulsars using their observed spindown rates, or limits. This method gives 10^8–10^9 G.

If the evolutionary connection between LMXBs and radio millisecond pulsars is correct, then working backward from the end result provides a different way to estimate LMXB spin periods. If an observed LMXB is in torque equilibrium, the current spin period of the LMXB progenitor is approximately the same as that of the radio pulsar it will later produce. The radio periods are mostly in the range 1.5–10 ms, and this range becomes the estimated LMXB period range as well. However, no fully satisfactory scenario currently exists which incorporates all details, including population statistics in globular clusters (Kulkarni, Narayan, & Romani 1990), of millisecond radio pulsars and LMXBs.

Consistency requires that there have been sufficient elapsed time to complete the required angular momentum transfer. The most conservative estimate of this time follows the scheme used by Wagoner (1984) who assumed a magnetic field less than 10^8 G, too weak to form a magnetosphere. Angular momentum transferred per unit accreted mass, dJ/dM, then assumes its lowest possible value. Wagoner estimated 0.4 $M_\odot$ must be accreted to reach spin periods of approximately 1 ms; this requires $10^{7.5}$–$10^{9.5}$ yr at an accretion rate of 10^{-8}–10^{-10} $M_\odot$ yr^{-1}. The estimated mass transfer requirement is an upper bound because spin periods of radio millisecond pulsars are often longer, up to several milliseconds, and also because a larger magnetic field than that used by Wagoner will increase dJ/dM without precluding evolution to a radio millisecond pulsar.

The common element in the foregoing parameter estimates is the standard disk magnetosphere interaction for which equation (1) gives the limiting spin period. Other limits may apply if μ is very small. The most rapidly spinning radio pulsars such as PSR 1937+21 and PSR 1957+20 suggest possible relevance of these other limits, which we now describe.

Two limits on spinup exist in the absence of a magnetic field. The better known one is the centrifugal breakup limit. There is also a general relativistic effect that can become significant at millisecond spin periods, one that has been recognized since the 1970s. This limit is associated with instabilities driven by gravitational radiation reaction (Chandrasekhar 1970; Friedman & Schutz 1978). Wagoner (1984) showed how these CFS instabilities could be excited in LMXBs and that the neutron star could become a pulsar in both gravitational waves and X-rays, with the frequency (common to both X-rays and gravity waves) being that of the rotating nonaxisymmetry responsible for the gravity wave emission, as seen in the inertial frame of the observer. This frequency is not the same as the stellar rotation frequency but is nevertheless expected to be in the range 200–800 Hz.

Spin period equilibrium is reached with the CFS mechanism when the gravitational instability growth time equals the viscous damping time. In equilibrium the angular momentum added to the star by accreting matter is radiated away in gravitational waves. The equilibrium equation analogous to equation (1) depends upon what nonaxisymmetric mode is excited; numerical results are given in Wagoner (1984) for reasonable values of the viscosity. Friedman, Ipser, & Parker (1986) have considered this scenario from the standpoint of the fastest radio millisecond pulsars and speculate that the 642 Hz spin frequency of PSR 1937+21 could be just below the threshold for exciting the CFS instability.

Whether or not the CFS mechanism limits spinup in LMXBs, it is desirable to search in X-ray time series for spin frequencies up to at least the 642 Hz frequency observed for the fastest radio millisecond pulsar. What are the highest limits that might be considered as outer bounds for period searching? Recently several papers have appeared exploring how neutron star spin frequencies up to 2 kHz might arise (Friedman et al. 1986; Michelson & Wood 1989). For the softest proposed equations of state, the only way to reach such high spin frequencies requires supporting the star by angular momentum, that is, if sufficient angular momentum were removed, the star would collapse to a black hole. There is presently no positive observational evidence to support spin frequencies this high and no basis for expecting them in the context of the standard picture of LMXBs, but the fact that they cannot be completely excluded with conventional equations of state shows that it is desirable to push pulsation searches to high frequencies, roughly 2 kHz.

A similar question may be posed for the low-frequency end: what is the minimum frequency that is approximately compatible with current understanding of LMXB sources? Circumstantial evidence cited earlier shows LMXB magnetic moments are probably well below 10^{28} G cm^3. If we conservatively use an upper bound of $\mu = 10^{29}$ G cm^3 in equation (1), we obtain an extreme upper limit of about 200 ms for bright LMXB and perhaps 500 ms for fainter ones. This limit is most relevant to sources that neither show HBO nor bursts, so that the other field estimates are not necessarily applicable. GX 9+1 is one example of such a source.

Several detections of possible periodicities should be mentioned. There have been at least five reported transient detections during X-ray bursts. In four cases the detection has been seen only once in the source in question; in one (the Rapid Burster) it was seen in two bursts at slightly different periods. The sources and periodicities are: MXB 1728−34, 12 ms (Sadeh et al. 1982); 4U 1254−69, 27 ms (Mason et al. 1980); Aql X-1, 130 ms (Kelley et al. 1989); the Rapid Burster, 503 and 508 ms (Tawara et al. 1982); and 4U 1608−52, 650 ms (Murakami et al. 1987). Periods seen only during bursts might have causes other than the spin of the star, such as oscillations in the burst envelope. The period in Aql X-1 shows no drift while those in MXB 1728−34 and 4U 1608−52 show substantial drift. A 2.93 ms pulsation in hard X-rays from Sco X-1 was reported by Leahy (1987). However, this period has not been seen in other observations of comparable or greater sensitivity (Middleditch & Priedhorsky 1986; Wood et al. 1989; this paper) and is almost certainly spurious.

2.2. *Caveats*

Uncertainties relating to the exact specification of magnetic field evolution were already described. Magnetic field estimates based on X-ray bursts and QPOs are vulnerable in part because neither bursts nor HBOs are seen universally in LMXBs, hence such estimates cannot rigorously be extended to all LMXBs. Doubts about validity of HBO models are another obvious concern. Recently Norris et al. (1990) have shown that the specific modulation mechanism suggested for the HBO may have difficulties explaining the lack of short time scale correlations between low-frequency noise and QPO strength; however, the possible relationship between QPO frequency and stellar spin frequency remains a promising aspect of the beat frequency model for HBO. One reason for searching for millisecond pulsars in sources that show HBO is to attempt to confirm the most basic assumption of the beat frequency model.

Extending field estimates obtained from a few members of a class to the entire class is justified only if the class is well defined and reasonably homogenous. The X-ray source classification scheme is still evolving. Two groups of LMXBs have now been identified based on differences in spectral modes and fast X-ray variability. These are the so-called Z sources (which show the horizontal branch oscillations and the approximately 6 Hz normal branch oscillations) and the atoll sources (Hasinger & van der Klis 1989; van der Klis 1989). Hasinger & van der Klis (1989) have suggested that the magnetic fields of the neutron stars in atoll sources are systematically different from those in Z sources, possibly related to a systematic difference in orbital periods and evolutionary histories. It may therefore be critical to avoid subclass boundaries in estimating source parameters. As an extreme type of class-related issue, it should be recalled that we have chosen to regard pulsation periods near 7 s in 4U 1626−67 and 1H 2259+586 as irrelevant to the LMXB spin period question. Although there is ample justification for this choice there is still room for it to be wrong since in at least 1H 2259+586 the field is estimated to be somewhat weak (Davis, Coe, & Wood 1989; Davies, Wood, & Coe 1990). In addition it is possible that the range of bottom fields of neutron stars is much larger than hitherto believed (Verbunt, Wijers, & Burm 1990; Bhattacharya & van den Heuvel 1990).

The synthesis of theoretical understanding for the QPO sources that follow the Z color-color diagram (Lamb 1989) uses three different geometries for the accretion disk and magnetosphere, one for each branch of the Z diagram. Equation (1) is sensitive to changes in geometry because its derivation involves estimating the radius of the magnetosphere. The picture of disk magnetosphere interaction that underlies equation (1) has been most fully validated for binary X-ray pulsars, that is, HMXB and not LMXB sources (Ghosh & Lamb 1979a, b; Angelini, Stella, & Parmar 1989). Certain anomalies remain to be explained even in HMXBs that exhibit QPOs, in that the fastness parameter and the sign of the period derivative are not in agreement with the predictions of the Ghosh and Lamb accretion torque model (Shibazaki 1989).

All aspects having to do with an evolutionary link to radio pulsars are tentative because there are alternative ways to account for the origin of those radio sources. An alternative scenario for some globular cluster millisecond radio pulsars involving accretion-induced collapse of white dwarfs has been proposed by Grindlay & Bailyn (1988); however, Verbunt, Lewin, & van Paradijs (1989) have shown that this hypothesis encounters a number of serious problems. Alternative scenarios involving stars with a common envelope are described by Rappaport (1989).

Ultimate limits on spin frequencies derived from the CFS instability or candidate equations of state for neutron star matter are theoretical constructs, with no direct observational confirmation.

Not all of these concerns are of the same weight. Individually, most of them translate into factors of only a few in uncertainty concerning the period. However, some can combine constructively with one another to spread the allowed period range. Note also that the range of 10^4 in HMXB spin periods—69 ms to 13 minutes—is produced by combining widely varying accretion conditions with a comparatively narrow range of field strengths. While the long periods of HMXBs are not those expected for LMXBs, the scatter in those periods might be relevant. The scatter in radio millisecond pulsar periods represents another estimate. We conclude that a thorough search for periods in LMXBs, while plausibly concentrating on the range from a few to 10 ms, must try to look at a much broader range, say 0.5–500 ms, in order to cover what our current knowledge allows.

2.3. *Drifts*

Discovery of faint coherent signals using Fourier transform methods depends upon having most of the power in a single channel of the transform. Frequency drifts are inimical to discovery unless they are known and can be removed in data analysis. Unknown drifts may be of two types in LMXBs: (1) intrinsic variation in the pulsar spin rate because of nonvanishing torques on the star and (2) drifts associated with orbital motion in the binary system. In the context of the standard accretion model (Ghosh & Lamb 1979a, b) applied using magnetic moments of 10^{27}–10^{28} G cm^3, the expected intrinsic drifts will be very small. If the source is near the equilibrium period given by equation (1), they will be totally negligible. In strong contrast, drifts associated with binary orbital motion prove to be an important barrier to detection of faint millisecond pulsations in LMXBs.

The basis for estimation of drifts is the knowledge of LMXB orbits. Parmar & White (1988) list 25 orbital periods for LMXB systems, ranging from 685 s for 4U 1820−30 to 9.8 days for Cyg X-2. The orbital period range and distribution for LMXBs resembles that for cataclysmic variables. A large theoretical literature exists on the origin of this distribution, including a well-known gap near orbital periods of 3 hr (e.g., Robinson 1983).

In every LMXB the available information on the orbit falls far short of what would be needed to correct for it in millisecond pulsar searches. In MXB 1659−29 and EXO 0748−676, orbital periods are now known to better than seven decimal places (Parmar et al. 1986; Cominsky & Wood 1989), and the center of eclipse serves as a good phase marker; however, even in these cases parameters such as the semimajor axis, inclination angle, and eccentricity are poorly constrained. The circularization resulting from gravitational radiation and tidal interactions at periastron is effective in reducing orbital eccentricity to a low value. Orbital periods determined optically can have several places of accuracy while those estimated from dips typically give only two or three places. Finally in many LMXBs the orbit remains totally unknown. It is assumed for the present work that unknown LMXB orbital periods are distributed roughly like the known ones. As remarked above already, there may be associations of orbital periods with particular subclasses. Among the six Z sources Sco X-1 and Cyg X-2 have known orbital periods, and both are relatively long (0.79 and 9.8 days, respectively). The known orbital periods among the atoll sources range between 0.2 and 8 hr.

The range of Doppler shifted drift rates that must be allowed for in millisecond pulsar searches follows from the known orbital periods and estimated semimajor axes. A long orbital period such as in Cyg X-2 will give drift rates of 2×10^{-9} s^{-1}, while a short period such as in 4U 1820−30 will give drifts of 3×10^{7} s^{-1}. With data segments 20 minutes long (typical of data obtained from satellites in low Earth orbit) the minimum orbital period that allows a pulse search using our method if the entire data set is used is approximately 3 hr (see § 4).

2.4. *Amplitudes*

Observational data and theoretical analysis provide some insight into expected pulse amplitudes. Previous searches for spin periods in LMXB sources include those done by Parsignault & Grindlay (1978), Córdova, Garmire, & Lewin (1979), Cominsky et al. (1980), Leahy et al. (1983), and Mereghetti & Grindlay (1987). Upper limits established in these searches were on the order of 4%–10% of the DC flux for periods longer than 1 s. Searches for periods much shorter than 1 s have yielded upper limits in the 0.3%–3% range (van der Klis et al. 1985; Middleditch & Priedhorsky 1986; Hasinger & van der Klis 1987; Stella, White, & Priedhorsky 1987; van Paradijs et al. 1988; Hasinger, Priedhorsky, & Middleditch 1989). The present authors have also published earlier partial results of the kind presented here, reaching limits as low as 1% (Wood et al. 1987; Norris & Wood 1987; Hertz et al. 1990). These results clearly show the desirability of searching below the 1% level of pulsation.

There has also been theoretical discussion of pulse amplitudes to be expected, much of it stimulated by the beat frequency model for HBOs. Low intrinsic modulation depth may prevail in LMXBs because the weak field is ineffective at channeling plasma flow to polar caps. In comparison with accretion columns in the high-mass binary systems, those near polar caps in LMXBs may be poorly defined. They may also be at lower altitudes and may cover a larger fraction of the stellar surface. These conditions will be unfavorable to high modulation depth. In addition several mechanisms for pulse suppression may operate in this environment including atmospheric scattering effects (Brainerd & Lamb 1987; Wang & Schlickeiser 1987; Bussard et al. 1988) and gravitational lensing (Wood, Ftaclas, & Kearney 1988; Mészáros, Riffert, & Berthiaume 1988). All of the above effects can operate simultaneously. Pulse suppression that depends on scattering in the hot material surrounding the neutron star can vary with the geometry. For the accretion geometries proposed by Lamb (1989) for the three branches of the Z diagram, it is likely that the horizontal branch is the most favorable to pulsar detection.

In the case where the CFS mechanism is excited, Kluźniak & Wilson (1987) give estimates as high as 10^{-3} for the pulsed fraction of X-rays produced by the accretion flow interacting with the nonaxisymmetric neutron star. The pulsed amplitude, considering all types of coherent signals, is thus highly uncertain; from previous searches, we know that it is unlikely to exceed 1%.

2.5. *Summary*

Spin periods expected in LMXBs are about 1–10 ms, but caution concerning the standard picture favors a broader search, from roughly 0.5–200 ms. Orbital velocities dominate expected frequency drifts; where the orbit is unknown the observed spin period drift, $P_{\rm spin}^{-1}\, dP_{\rm spin}/dt = \nu^{-1} d\nu/dt$, can be anywhere from zero up to $3 \times 10^{-7}\ {\rm s}^{-1}$. The fractional pulsed amplitude, A, is expected to be less than 1%. For particular sources it may be appropriate to constrain the search using what is known of the binary orbit or by trying to observe it in a mode of activity favorable to pulse detection. It is not possible to search the full volume of interest in ($P_{\rm spin}$, $dP_{\rm spin}/dt$, A) space using *Ginga* and *HEAO 1* data, but it is possible to search regions that have never been searched before, thereby reducing limits on A to less than 1% for a few of the brightest sources and for a large portion of the interesting range in $P_{\rm spin}$ and $dP_{\rm spin}/dt$.

3. COHERENCE RECOVERY TECHNIQUE

Arrival times of pulses from a binary pulsar are delayed or advanced by source motion along the line of sight. Uncorrected accelerations appear as period drifts and reduce the time over which coherence can be maintained in Fourier transforms. Incoherent summation of power spectra from short data segments is far less sensitive for finding faint pulsed signals than the optimal signal to noise achieved if coherence can be maintained over the full duration of the available data. In principle this can be done by removing accelerations from the data using a redefinition of the time coordinate followed by Fourier transforming the rebinned data. Lost coherence could be recovered for pulsars in LMXBs—given unlimited computational resources—by a trial and error search of all realistic binary orbits. For circular orbits this means searching a three-dimensional phase space of orbital radius, orbital frequency, and phase. With a general elliptical orbit there are five parameters. The computational cost of this procedure becomes prohibitive because it scales with integration time $T_{\rm int}$ as approximately $T_{\rm int}^7$ for three parameters (Wood et al. 1987).

If $T_{\rm int}$ is much less than the orbital period $P_{\rm orb}$, the exact sinusoidal correction to pulse arrival time may be approximated acceptably by expanding to second order in a power series. This reduces the unknown orbital parameter space from three dimensions to one, saving orders of magnitude in computational cost. This procedure is the optimum single parameter coherence recovery technique (CRT), applicable when there is complete or near-complete ignorance of orbital parameters. A CRT search can be performed in the time domain using a family of quadratic time transformations to rebin the original time series, followed by a Fast Fourier Transform (FFT) for each rebinning. The number of time transformations required to search a fixed range of orbits now scales roughly as $T_{\rm int}^3$, which is manageable up to integrations of a few thousand seconds with millisecond data bins. Alternatively, CRT can be performed in the frequency domain by computing an optimal linear filter for each quadratic transformation while performing the FFT of the signal only once (see Appendix A). The sensitivity and end results for both methods are identical.

The details of CRT implementation in the time domain are described in the remainder of this section. The defining approximations and the search grid are specified. Limitations on use of CRT in the time and frequency domains are given, with assessment of relative merits of the two approaches. We also compare the sensitivity achievable for CRT with that of the method of incoherent summations of short FFTs. In some cases precise information about the orbit affords the possibility of two-parameter searches that can extend integration times beyond those possible with single parameter CRT. We describe two special cases of this kind.

3.1. *Coherence Recovery in the Time Domain*

Let the varying distance between the solar system barycenter and the source be given by $D(t)$ in the observer's frame. Slow acceleration of the binary system with respect to the Sun is neglected. Only the periodic component due to orbital motion is treated. A photon emitted by the source at time t' is received at the detector at time t given by

$$t = t' + D(t)/c\ , \tag{2}$$

where c is the speed of light. The emitted signal is assumed periodic in the source rest frame, with period $P_{\rm pul}$.[3] Intrinsic period drifts are small compared to those associated with the orbit, but if they were large enough to be of interest, the method would accommodate them. The derivative $dP_{\rm pul}/dt$ would add small contributions to the first three terms in the expansion of $D(t)$, in equation (4) below.

Leahy et al. (1983) compared pulsar searches conducted with phase histograms and FFTs. If the pulsar waveform is reasonably close to a sinusoid, the FFT is a much better compromise between sensitivity and computation cost. We assume that the signal is essentially sinusoidal. Ignorance concerning $D(t)$ must be overcome by searching a grid sufficiently dense that some element of the grid concentrates power near the fundamental into one channel of the power spectrum.

We derive the one-dimensional search grid for circular orbits. The circular approximation is used because (1) as noted in § 2, orbits in LMXBs should be close to circular, (2) it simplifies the notation, and (3) the procedure for rebinning and transforming is unaffected by details of how the quadratic coefficient is expressed in terms of orbital parameters.

The maximum advance or retardation of pulse arrival time is given by $a_\perp = a \sin(i)/c$, where a is the orbital radius and i is the inclination angle; $a_\perp$ is the projected orbital radius expressed in light seconds. If the binary system revolves with angular frequency $\Omega_{\rm orb} = 2\pi/P_{\rm orb}$, then the advance or retardation of the pulse phase $\delta\phi_{\rm pul}$ is given by

$$\begin{aligned}\delta\phi_{\rm pul} &= \omega_{\rm pul} D(t)/c \\ &= \omega_{\rm pul} a_\perp \sin(\Omega_{\rm orb} t + \phi_0) ,\end{aligned} \tag{3}$$

where $\omega_{\rm pul} = 2\pi/P_{\rm pul}$ is the angular frequency of the pulsed signal and ϕ_0 is the orbital phase at time $t = 0$. Note that ϕ_0 is measured from quadrature. Expanding $\delta\phi_{\rm pul}$ to second order in powers of t about $t = 0$ gives

$$\begin{aligned}\delta\phi_{\rm pul} = {} & a_\perp \omega_{\rm pul} \\ & \times [\sin(\phi_0) + \Omega_{\rm orb} \cos(\phi_0)t - \tfrac{1}{2}\Omega_{\rm orb}^2 \sin(\phi_0)t^2] .\end{aligned} \tag{4}$$

The second term in equation (4) represents an average Doppler shift for the interval of observation. This term does not broaden the peak in the power spectrum since it is linear in time; however it may shift the peak to another frequency bin. The third term, in which phase is quadratic in time so that frequency broadens linearly with time, constitutes the lowest order broadening effect in frequency space. This term attains its greatest magnitude when the argument of the sine is $\pm\pi/2$.

We define a new time coordinate, t_α, in which phase delays are (nearly) compensated:

$$\begin{aligned}t_\alpha &= t + \tfrac{1}{2} a_\perp \Omega_{\rm orb}^2 \sin(\phi_0)t^2 \\ &= t + \alpha t^2 ,\end{aligned} \tag{5}$$

where $\alpha \equiv a_\perp \Omega_{\rm orb}^2 \sin(\phi_0)/2$. The new time coordinate t_α was derived as the coordinate in which the dependence of pulse phase, $\phi_{\rm pul} = \omega_{\rm pul} t + \delta\phi_{\rm pul}$, on time is (nearly) linear. At most orbital phases, the first neglected term in the expansion of equation (3) approximates the instantaneous residual phase error, $E(\phi)$. This term is representative of the typical error when the orbit is unknown:

$$E(\phi) = \tfrac{1}{6} a_\perp \omega_{\rm pul} \Omega_{\rm orb}^3 \cos(\phi_0)t^3 . \tag{6}$$

Numerical simulations show that more than 90% of the pulse fraction is recoverable in principle for all orbital phases if $T_{\rm int} < P_{\rm orb}/4\pi$, provided the α-grid is sufficiently dense (see § 3.3). The search algorithm is now clear: for each value of α, we perform a time transformation on the data, as in equation (5), followed by a FFT.

3.2. *Grid Characteristics for Binary Orbits*

We now derive the critical increment for the quadratic parameter α and express the extreme values of α in terms of orbital parameters. We then estimate the effective number of independent frequencies searched in performing the full set of quadratic transformations, a quantity needed to determine the sensitivity of the technique for faint signals.

Consider a signal with period $P_{\rm pul}$ broadened over two bins in the power spectrum by frequency drift. We wish to find the increment $\delta\alpha$ which will recover all power in one bin. For this purpose let us assume the α approximation is exact. The phase lag $\delta\phi_{\rm pul}$ in a pulsed signal at frequency $\nu_{\rm pul} = 1/P_{\rm pul}$ caused by a time delay αt^2 will be

$$\delta\phi_{\rm pul} = 2\pi\alpha t^2 \nu_{\rm pul} , \tag{7}$$

and the frequency broadening associated with this accumulating phase residual over the interval $[0, T_{\rm int}]$ will be

$$\begin{aligned}\delta\nu &= \frac{1}{2\pi} \frac{d^2(\delta\phi_{\rm pul})}{dt^2} T_{\rm int} \\ &= 2\alpha\nu_{\rm pul} T_{\rm int} .\end{aligned} \tag{8}$$

The frequency interval corresponding to a shift of one channel in the power spectrum is $\nu_{\rm Nyq}/N_f$, where N_f is the number of bins in the power spectrum or half the number of data points, the Nyquist frequency is $\nu_{\rm Nyq} = 1/(2\tau)$, and τ is the width of a time bin. The bin width in frequency space is $1/T_{\rm int}$. We want $\delta\nu_{\delta\alpha}$, defined as the frequency expansion or compression associated with going from α to $\alpha + \delta\alpha$, to correspond to the width of one power spectrum channel, that is, $1/T_{\rm int}$, hence

$$\begin{aligned}\frac{1}{T_{\rm int}} &= \delta\nu_{\delta\alpha} \\ &= \frac{d(\delta\nu)}{d\alpha} \delta\alpha \\ &= 2\nu_{\rm pul} T_{\rm int} \delta\alpha ,\end{aligned} \tag{9}$$

or

$$\delta\alpha = \frac{1}{2\nu_{\rm pul} T_{\rm int}^2} . \tag{10}$$

Because we do not know the pulse frequency, the worst case value, $\nu_{\rm Nyq}$ must be used. This means that at frequencies much lower than the Nyquist frequency there is oversampling, as described below.

Inspecting equation (5) we find that the extreme values of α occur when $\sin(\phi_0) = \pm 1$, that is, at the times when the source is at opposition or conjunction and its velocity is perpendicular to the line of sight. The grid must be large enough to cover this case, hence the largest value of the quadratic parameter which must be searched is

$$\alpha_{\max} = a_\perp \Omega_{\rm orb}^2/2 , \tag{11}$$

[3] The CRT method described here does not require that pulses be due to a spinning neutron star, hence the distinction between $P_{\rm pul}$ and $P_{\rm spin}$ in this section.

and the total number of quadratic transformations which must be performed is

$$N_\alpha = 2\alpha_{\max}/\delta\alpha$$
$$= 2a_\perp \nu_{\rm Nyq} \Omega_{\rm orb}^2 T_{\rm int}^2 \,. \qquad (12)$$

The quadratic dependence on integration time in equation (12) combined with the fact that the number of operations in the FFT scales as $T_{\rm int} \log_2 (T_{\rm int})$ justifys the statement made earlier that the computational cost of this one-dimensional CRT scales roughly as $T_{\rm int}^3$.

From Kepler's third law the semimajor axis of the neutron star orbit is

$$a_\perp = 1.175\mu_{\rm comp}(P_{\rm orb}/1\ {\rm hr})^{2/3}(M_{\rm tot}/M_\odot)^{1/3} \sin (i)\ {\rm lt\text{-}sec}\ , \quad (13)$$

where $M_{\rm ns}$ and $M_{\rm comp}$ are the masses of the neutron star and binary companion, respectively, $M_{\rm tot} = M_{\rm ns} + M_{\rm comp}$ is the total mass of the binary system, and $\mu_{\rm comp} = M_{\rm comp}/M_{\rm tot}$ is the mass fraction of the companion. The maximum value for α in terms of these parameters is

$$\alpha_{\max} = 1.79 \times 10^{-6}\mu_{\rm comp}(P_{\rm orb}/1\ {\rm hr})^{-4/3}(M_{\rm tot}/M_\odot)^{1/3}\ {\rm s}^{-1}\ . \quad (14)$$

The number of independent frequency and acceleration combinations in all power spectra covered in the grid, $N_{\rm tot}$, is needed to evaluate the probability of detected signals and establish modulation levels corresponding to upper limits. This number is a function of signal strength. Near threshold it is straightforward to estimate. The increment in the quadratic parameter, $\delta\alpha$, was chosen such that the N_α searches for pulsations are independent for a signal at the Nyquist frequency. From equations (10) and (12), it is clear that the number of independent accelerations at some other frequency ν_j is $(\nu_j/\nu_{\rm Nyq})N_\alpha$. More α-values than that may be computed in the grid, but frequency-dependent redundancy is required at lower frequencies in order to achieve the needed grid density at the Nyquist frequency. For the frequency ν_j corresponding to the jth bin in the power spectrum, $\nu_j = j/T_{\rm int}$ and $\nu_j/\nu_{\rm Nyq} = j/N_f$. The total number of combinations at all frequencies is then

$$N_{\rm tot} = \sum_{j=1}^{N_f} N_\alpha(j/N_f)$$
$$= N_\alpha(N_f + 1)/2\ , \qquad (15)$$

or, to good approximation,

$$N_{\rm tot} = N_\alpha N_f/2\ . \qquad (16)$$

In using equation (16) it is essential to recognize that the CRT method is necessary only when the signal is faint enough that pulse broadening from orbital modulation renders the signal power small compared to the noise level produced by Poisson fluctuations. Adjacent frequency channels are strictly independent (orthogonal) in any of the individual power spectra produced for a particular value of α, but no analogous independence exists between power spectra in the sequence of quadratic time transformations, that is, when ν is fixed and α is varied. One can appreciate the point by considering strong signals. If a strong, strictly periodic signal is present at the central frequency of channel i, no excess power is seen in the adjacent channel $i + 1$. However, if a quadratic time transformation characterized by α is applied to the same data, the signal in channel i will persist to very high values of α. Without noise, the signal would persist to *arbitrarily* high values of α. If a noise fluctuation were able to give such large power, it would necessarily also show up in many of the $N_{\rm tot}$ trials, reducing the effective number of independent trials in which to produce such a large spurious signal.

Equation (16) can be used to determine rigorously the threshold detectable signal at a given statistical significance. Since no incoherent summations of power spectra are performed, the power in each of the N_α spectra is distributed as χ^2 for 2 degrees of freedom ($\nu_{\rm dof} = 2$). For an FFT power spectrum of Poisson-distributed fluctuations, with local power normalized to unity, the probability that the power spectrum amplitude in any frequency bin exceeds power P is e^{-P}. The probability of no power spectrum amplitude exceeding P in $N_{\rm tot}$ independent searches is

$$Q(\chi^2 > P) = 1 - (1 - e^{-P})^{N_{\rm tot}} \simeq N_{\rm tot} e^{-P}\ . \qquad (17)$$

If a signal is actually detected using CRT and is considerably higher than threshold, the chance expectation calculated using equation (17) will be a conservative estimate (overestimate) of the true chance expectation. In fact, the correct value of $N_{\rm tot}$ will decline as signal strength increases, reaching an asymptotic limit of N_f for very strong signals, that is, those that could have been detected without α-shifting no matter what the orbital parameters were.

3.3. *Determination of Pulse Amplitude Limits*

It is necessary to express detected signals in terms of their chance expectation of occurrence, whereas upper limits must be expressed as fractions of the source DC level. This problem has been treated by Leahy et al. (1983). What follows is the adaptation of their general formulae to the CRT situation, including treatment of the number of independent frequency and acceleration combinations.

In the absence of a detected signal we determine the search sensitivity by calculating the expected power obtained from a sinusoidal signal of average intensity r_0 and modulation depth A, that is, $r(t) = r_0[1 + A \sin (\omega_{\rm pul} t + \phi_0)]$. In calculating P_j, the power in the jth power spectrum bin, we adopt the normalization

$$P_j = \frac{1}{N_\gamma} |a_j|^2\ , \qquad (18)$$

where the complex Fourier amplitudes a_j are given by

$$a_j = \sum_{k=1}^{N} X_k e^{i\omega_j t_k}\ . \qquad (19)$$

Note that this normalization is half the normalization adopted by Leahy et al (1983). Here X_k is the number of counts in data bin k of the light curve, $t_k = k\tau$ is the time of the kth light curve bin, $\omega_j = 2\pi\nu_j = 2\pi j/T_{\rm int}$ is the frequency of the jth frequency bin, $N = 2N_f = T_{\rm int}/\tau$ is the number of data bins, and N_γ is the total number of photons in the data set. In practice the mean count rate is usually subtracted from the data X_k. Leahy et al. (1983) calculate the expectation value of the power in the power spectrum bin with frequency ω_j closest to the signal frequency $\omega_{\rm pul}$, taking into account the loss in power due to finite binning and the expected mismatch between signal frequency and any of the discrete frequencies searched by the FFT. Using our normalization the expectation value $\langle P_j \rangle$ for a single FFT is

$$\langle P_j \rangle = 1 + 0.773 N_\gamma \frac{A^2}{4} \frac{\sin^2 (\omega_j T_{\rm int}/4N_f)}{(\omega_j T_{\rm int}/4N_f)^2}\ . \qquad (20)$$

We choose the modulation depth A such that 95% of the time χ^2 exceeds a value P. Also the chance expectation to exceed P (in N_{tot} frequency times acceleration trials) is set equal to $1 - 0.95$. These choices correspond to $C' = C = 0.95$ in the notation of Leahy et al. (1983). Following the prescription given there for solving for the amplitude and using the simplification that $Q(\chi^2 > P) = \exp(-P)$ for our case, the first estimate of the upper limit to the pulse amplitude at frequency ω is

$$A_0(\omega) = \left[\frac{5.2}{N_\gamma}\frac{(\omega T_{int}/4N_f)^2}{\sin^2(\omega T_{int}/4N_f)}\log\left(\frac{0.5N_f N_\alpha C'}{1-C}\right)\right]^{1/2} \quad (21)$$

(see also Lewin et al. 1988, § 2.2.2).

$A_0(\omega)$ is not the quantity we require because there are further correction factors for power lost to approximations in CRT. Because we use discrete values of the search parameter α, we must account for the possibility that the optimum value of α differs from any value in our trial sequence by an amount $\Delta\alpha$, and then average over values of $\Delta\alpha$. This calculation is performed in Appendix B. The expected loss of power is frequency dependent and grows with frequency. The upper limit on modulation depth is $A(\omega) = A_0(\omega)A_{loss}(\omega)$, where $A_{loss}(\omega)$ is the desired correction factor. For small values of frequency, $A_{loss}(\omega)$ is near unity. It achieves its maximum value of approximately 1.1 at the Nyquist frequency.

There are two additional effects that must be taken into account. These may best be described as incomplete signal recovery. First, even if the actual value of α for a particular orbit falls exactly on a trial α value, we do not completely recover the signal because we are approximating a sinusoid with a quadratic. Second, we suffer additional loss of power because of information lost when we rebin data before performing the FFT.

The power lost from both of these additional effects has been evaluated with numerical simulations. In the simulations, pulsations with known pulse fraction A and frequency ω_{pul}, and with sinusoidal frequency variations of known frequency Ω_{orb} and phase ϕ_0, were placed in a data set and recovered using CRT, that is, with a quadratic approximation to the sinusoidal orbit. The data is rebinned by assigning the counts in the original bin centered at time t to the transformed bin centered at time t_α. This binning scheme, as opposed to dividing the counts in the original bin among two transformed bins, preserves the Poisson characteristic of the data.

The simulations reveal several subtleties of CRT. First, the best value of α, that is, that value for which the recovered pulse fraction A_{rec} is highest, is slightly different from the theoretical best α given by equation (5). The difference in α is typically less than 1%, but can be a few times $\delta\alpha$. This is because the best α minimizes the total error introduced by the quadratic approximation to the sinusoidal frequency modulation, not just the error in the quadratic term of the expansion of the sinusoid. Thus the error term given in equation (6) is an upper limit to the error in the best quadratic approximation.

Second, the quadratic approximation becomes progressively worse as the fraction of the orbit traversed by the pulsar during the observation increases. We find that A_{rec} exceeds 90% at all orbital phases as long as $T_{int} < P_{orb}/4\pi$. For long integration times, A_{rec} drops quickly. Third, for a fixed ratio T_{int}/P_{orb}, A_{rec} is a function of the orbital phase ϕ_0 at which the observation is made. From equation (6) we see that $E(\phi_0)$, the residual error from the quadratic approximation, is minimized at stellar conjunction or opposition ($\phi_0 = \pm\pi/2$). The maximum error due to the quadratic approximation occurs at quadrature ($\phi_0 = 0$). We show this effect in Figure 1. Here we have plotted, for various orbital phases, the difference between the quadratically corrected pulse period and the true pulse period during the observation. For these simulations, we have taken $M_{comp} = 0.6$ $M_\odot$, $M_{ns} = 1.5$ $M_\odot$, $P_{orb} = 3$ hr, $P_{pul} = 4.3$ ms, $\tau = 1$ ms, and $T_{int} = 10^3$ s. The pulse period difference is calculated for four orbital phases ranging from $\phi_0 = 0$ to $\pi/2$; here ϕ_0 is measured at the center of the observation. In Figure 1*a* we use the predicted α from equation (5), while in Figure 1*b* we use the best-fitted α.

The final effects result from rebinning of the data using the quadratic time transformation of equation (5) and is a function of both frequency, ω_{pul}, and quadratic coordinate, α. The rebinning loss is small compared to the loss due to the finite binning of the initial data, which is included in A_0 (see eq. [21]). In our simulations the additional loss due to rebinning as a function of ω_{pul} was negligible. This loss also depends on α, varying approximately linearly with α, or sinusoidally with phase (eq. [5]), but it is small, being less than 3% for simulations with $T_{int} < P_{orb}/4\pi$.

Figure 2 illustrates the increase in sensitivity of CRT over the method of incoherent summation (IS) of short FFTs, for the case when the orbit is unknown. Figure 2*a* shows the sensitivity achievable with the IS method as a function of M, the number of FFTs summed, for a fixed total data length, $N = 2^{20} \simeq 10^6$. In the absence of a signal, the left ordinate, χ^2, is the threshold power needed to exceed a 2 σ chance expectation level; this takes into account the number of candidate frequencies in the incoherently summed power spectrum. χ^2 is essentially the average noise power normalized to unity (see Leahy et al. 1983 for a detailed discussion). Thus the expectation value is

$$E_{IS} = N_f\, Q(\chi^2/\nu_{dof} = 2M)\,, \quad (22)$$

where $N_f = N/M$ is the number of frequency bins in each individual FFT. The corresponding limit on pulse fraction A attainable is shown on the right ordinate for a sinusoidal signal. The upper limit obtained for A for a given expectation level with associated χ^2 and total counts N_γ is (ignoring effects of finite binning)

$$A(E_{IS}) = 2\sqrt{\frac{(\chi^2 - 2M)/2}{N_\gamma/M}}\,, \quad (23)$$

where χ^2 is that in equation (22). At larger M the increase in sensitivity is less dependent on M, a conclusion apparent from the asymptotic approximation for χ^2 for many degrees of freedom (e.g., eq. [26.4.13] of Abramowitz & Stegun 1968). Figure 2*b* illustrates the sensitivity of CRT as a function of total points N for one long FFT and for the same expectation level and signal strength as in Figure 2*a*. In this case

$$E_{CRT} = N_{tot}\, Q(\chi^2 \mid \nu_{dof} = 2)\,, \quad (24)$$

and the associated upper limit obtained for A is

$$A(E_{CRT}) = 2\sqrt{\frac{\chi^2 - 1}{N_\gamma}}\,. \quad (25)$$

As can be seen from Figure 2, achievable sensitivity is greatly enhanced with long coherent FFTs, even taking into account the larger number of independent frequencies and α values. No effects of finite binning as described by Leahy et al (1983) are incorporated in Figure 2.

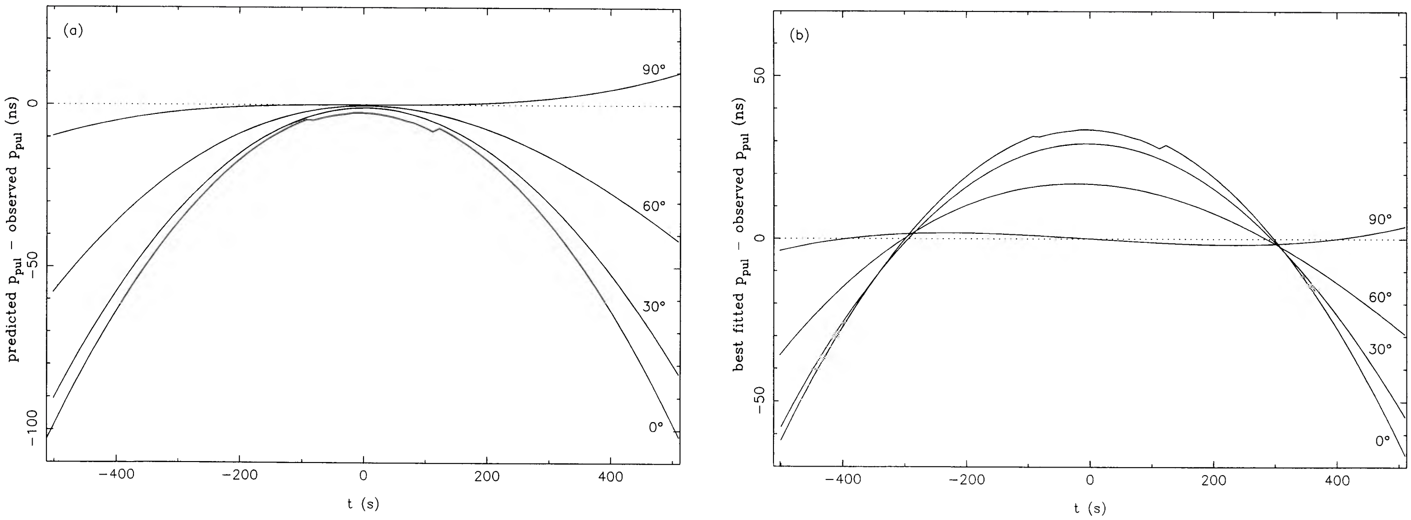

FIG. 1.—Residual error in predicted pulse period due to quadratic approximation of sinusoidal variation in frequency. The difference between the predicted pulse period and the true pulse period is plotted for (*a*) the quadratic parameter α given in eq. (5) and (*b*) the best-fitted quadratic parameter α. Period differences are plotted as a function of time during a 1024 s observation for four different orbital phases. Details of the calculation are given in the text. Small notches in the curves are due to computational roundoff errors.

The search of possible binary orbits can also be implemented in the frequency domain (see Appendix A). It involves taking only a single FFT of the data and generating all of the power spectra for the α-variation in the frequency domain. For the applications to X-ray pulsar searching, the time domain approach is computationally more efficient.

3.4. *Searches with Partial Knowledge of the Orbit*

A well-established orbital period and phase reference make possible two-parameter searches with integration times of order twice those possible using one-parameter CRT. A technique for performing such searches is by means of a cubic time transformation taken at quadrature, when the quadratic term vanishes.

Equation (3) gives the phase delay caused by a circular orbit. At quadrature, $\phi_0 = 0$ or π. Taking $\phi_0 = 0$ and expanding arrival time t' about $t = 0$ we obtain

$$t' = t + a_\perp \sin(\Omega_{\rm orb} t) \tag{26a}$$

$$= t + a_\perp \Omega_{\rm orb} t - \tfrac{1}{6} a_\perp \Omega_{\rm orb}^3 t^3 + \tfrac{1}{120} a_\perp \Omega_{\rm orb}^5 t^5 + \cdots \tag{26b}$$

$$\simeq t + \beta t^3 \,. \tag{26c}$$

Once again we have ignored the linear term since it introduces no frequency broadening. We can recover coherence with a sequence of β values. Varying β is essentially the same as varying the projected orbital radius $a_\perp$ through a sequence of values.

Even for a source with a precisely determined orbital period there is a small uncertainty in phase, making it necessary as a practical matter to search a grid of trial ϕ_0 values as well as β-values. The ϕ_0 grid spacing is determined by considering equation (3) with $|\phi_0| < \delta\phi$. One obtains the grid spacing for β or $a_\perp$ from equations (26b) and (26c) by the same method that

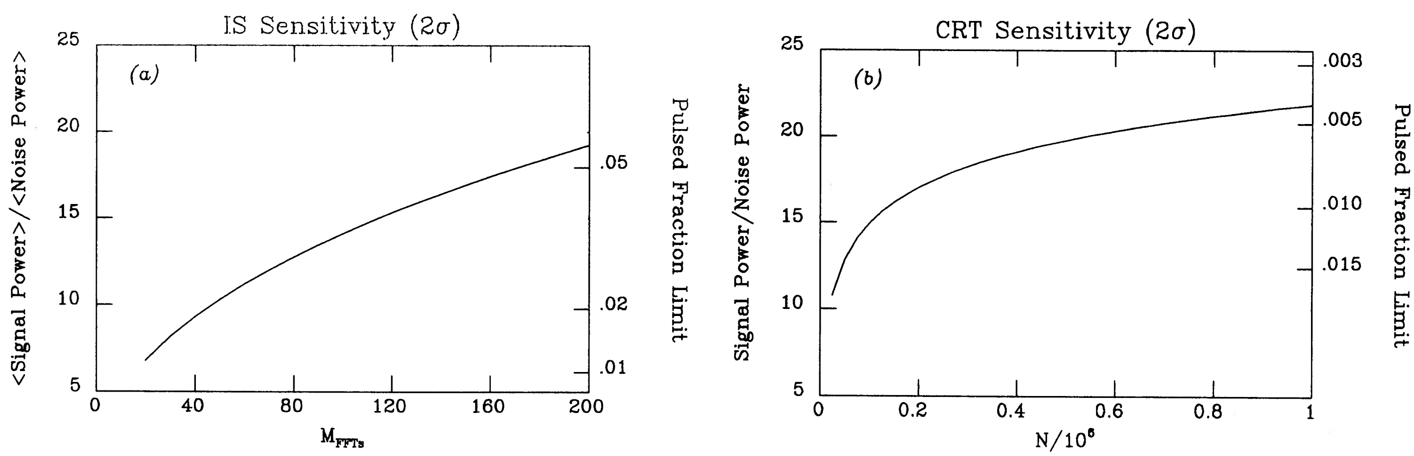

FIG. 2.—Sensitivity to pulse fraction (*a*) for incoherently summed FFTs and (*b*) for the method of trial quadratic time transformations (CRT), both for 2 σ detection criterion (*see text*). Values on right ordinates are for an assumed count rate (5000 count s^{-1}) typical of a bright LMXB source observed with *Ginga*'s LAC experiment.

was used to find $\delta\alpha$ in α-shifting CRT. The results are

$$\delta\phi = \frac{1}{a_\perp \beta \Omega_{\rm orb}^2 \nu_{\rm Nyq} T_{\rm int}^2} \tag{27}$$

and

$$\delta\beta = \frac{1}{3\nu_{\rm Nyq} T_{\rm int}^3} . \tag{28}$$

The number of $a_\perp$ (or β) values is found by calculating maximum and minimum reasonable radius values. Note that if we do not know whether the source is moving toward or away from us, then it is necessary to consider both positive and negative $a_\perp$ or β-values; if we do know, then the size of the search grid is cut in half. These relations also assume a circular orbit. Significant eccentricity will limit the practical integration time or force search of a larger grid.

A special case of another kind is that of 4U 1820−30, where a short and well-determined orbital period again makes search of a grid in $a_\perp$ and ϕ_0 a practical possibility. In this instance the data extend over many orbital periods so that one must use equation (26a) and not the cubic approximation in equation (26c). Equation (26a) is still valid and the increment of $a_\perp$ is given by

$$\delta a_\perp = \frac{3}{\Omega_{\rm orb}^3 \nu_{\rm Nyq} T_{\rm int}^3} . \tag{29}$$

4. OBSERVATIONS AND RESULTS

4.1. *Observations*

We have searched for millisecond pulsations with drifts in several low-mass X-ray binaries by applying the coherence recovery technique (CRT) to high time resolution data obtained with proportional counter arrays on board the *HEAO 1* and *Ginga* satellites. The *Ginga* data provide long data segments on several LMXBs at 1 ms time resolution. The *HEAO 1* data provide supplementary data segments with time resolution of 7 μs in the primary data, binned up to 300 μs for the present searches.

All *Ginga* data used in this study were taken in the PC telemetry mode at high bit rate during pointed observations with the Large Area Counter (LAC) array (Makino 1987; Turner et al 1989). The LAC consists of eight sets of proportional counters in two groups, LAC-A and LAC-B, which together provide a total effective area of 4000 cm^2. The energy bandpass is set separately for LAC-A and LAC-B, each of which has one high- and one low-energy channel in PC mode. Low-energy-channel data are stored in 1 ms bins and high-energy-channel data in 2 ms bins in the onboard Bubble Data Recorder (BDR). The BDR can store up to 42.3 minutes of data at high bit rate. The data rate is limited by the telemetry that can be transmitted and received during 10 minute contacts with the ground station in Kagushima, Japan; contacts occur five times daily.

Sco X-1, GX 5−1, Cyg X-2, GX 340+0, GX 17+2, and GX 9+1 were the *Ginga* targets used in this study. All are bright LMXBs, and all except GX 9+1 are QPO sources of the Z type (Hasinger & van der Klis 1989). In each of these sources it was possible to obtain at least 2^{20} points of continuous data and sometimes more. In Table 1A we give specifics of the observations.

During the 1977–1979 *HEAO 1* mission the *HEAO* A-1 Large Area Sky Survey (LASS) Experiment was used for pointed observations in addition to its primary scanning work. Modules 1–6 of the LASS instrument were located on the −Y

TABLE 1

A. Log of *Ginga* Observations[a]

Source	Observation Date	Count Rate (s^{-1})	Fujitsu N_α	Fujitsu $T_{\rm int}$ (s)	Connection Machine N_α	Connection Machine $T_{\rm int}$ (s)
Sco X-1	1989 Mar 9	14000	100	1024	121	2048
	1989 Mar 10	10000	100	1024	121	2048
GX 340+0	1988 Mar 30	2200	215	1024	...	...
	1988 Apr 6	2200	215	1024	...	...
GX 5−1	1987 Apr 20	7000	215	1024	2957	2048
	1987 Apr 27	5000	857	2048	2957	2048
GX 9+1	1988 Mar 29	3000	215	1024	...	...
	1988 Mar 31	3250	215	1024	...	...
GX 17+2	1988 Mar 28	3500	215	1024	...	...
	1988 Apr 1	2700	215	1024	...	...
Cyg X-2	1987 Jun 7	3400	7	1024	...	...
	1987 Jun 8	3400	7	1024	...	...

B. Log of *HEAO 1* Observations

Source	Observation Date	Count Rate (s^{-1})	τ (ms)	N_α	$T_{\rm int}$ (s)
4U 1820−30	1978 Oct 6	2075	5	960[b]	1310
Cyg X-3	1978 Jun 1	265	0.3	90	164
	1978 Dec 2	425	5	1080	2620
Cyg X-2	1978 Dec 1	2800	5	4	2620

[a] τ = 1 ms for all *Ginga* observations.

[b] Number of transformations is $N_A \times N_\phi$ for 4U 1820−30.

side of *HEAO 1* while module 7, which was coaligned with the *HEAO* A-2, A-3, and A-4 experiments, was located on the +Y side. Module 7, used for the observations included here, provided 1900 cm^2 of open collecting area with sensitivity between 0.25 and 25 keV. For the present observations, gain and discriminators were set so that the effective bandpass was 0.5–25 keV. *HEAO* A-1 was able to obtain long data segments with 5 ms timing resolution and could obtain shorter segments, up to 10 minutes, with a high bit rate that provided 7 μs timing resolution. The instrument itself is described in Wood et al. (1984) while further detail on the high time resolution telemetry features used for these searches may be found in Meekins et al. (1984).

The *HEAO 1* searches reported here cover three objects in which partial knowledge of the binary orbit is available. These are Cyg X-2 ($P_{orb} = 9^d.8$), Cyg X-3 ($P_{orb} = 4.8$ hr), and 4U 1820−30 ($P_{orb} = 685$ s). The Cyg X-2 period is established optically while the others are observed in X-rays.

4.2. *Simulations*

As discussed in § 3.3, we performed extensive simulations of pulsars in binary systems in order to verify both our technique and our programs. In the simulations, pulsations with known pulse fraction A and P_{pul}, and with sinusoidal frequency variations of known period P_{orb} and phase ϕ_0, were placed in a data set. The expected count rate was determined and used as the mean in a Poisson deviate generator. The data was generated with bin size τ comparable to the data sets analyzed.

A total of 55 simulated data sets were generated. For these simulations the range of parameters used was $\tau = 1/1024$ ms, $P_{orb} = 0.95$–30 hr, $P_{pul} = 1.9$ ms—1 s, $A = 0.03$, and $\phi_0 = 0 - \pi/2$. We set the integration time at $T_{int} = 1024$ s and the mean count rate at $r_0 = 25$ count bin^{-1}. In every case, the recovered frequency and amplitude was as expected. See § 3.3 for complete details of the simulations.

4.3. *Results*

Data analysis for *Ginga* observations was conducted using computers at the Institute for Space and Astronautical Science in Sagamihara, Japan, and at the Naval Research Laboratory, Washington, DC. Using standard FFT algorithms it was possible to perform 2^{20} point FFTs in approximately 11 s and 2^{21} point FFTs in 25 s with the Fujitsu computers at ISAS. Using the Connection Machine CM-2 at NRL it was possible to perform 2^{20} point FFTs in 0.9 s and 2^{22} point FFTs in 3.6 s. The implementation of the CRT algorithm on the Connection Machine utilizes the parallel architecture of that machine and is described elsewhere (Hertz 1990; Hertz et al. 1990). *HEAO 1* data was analyzed using a VAX 11/785 at NRL.

For Sco X-1 and Cyg X-2 the known orbital periods ($0^d.787$ and $9^d.8$, respectively) were used to constrain the number of values of α. With the exception of 4U 1820−30, the orbit was unknown for the other sources, and α_{max} was selected to allow for the shortest period orbits consistent with the length of the data stream, that is $P_{orb} \gtrsim 4\pi T_{int} \simeq 3$ hr for 1024 s data segments. While MXB 1916−05 ($P_{orb} = 50$ minutes) and 4U 1820−30 ($P_{orb} = 685$ s) have orbital periods shorter than this limit, most known LMXB orbital periods are consistent with it. For 4U 1820−30 itself a search was done using the methods derived for that special case in § 3.4. To allow for orbital periods as short as that of 4U 1820−30 in the sources with unknown orbits would require using much shorter data segments.

No millisecond pulsations were seen. Table 2 gives upper limits obtained for each source at the chosen 95% confidence level. The best upper limits obtained in the range below 10 ms were several tenths of a percent, in GX 5−1 and Sco X-1. The next section discusses implications of these limits.

5. DISCUSSION

In § 2 we summarized the basis for the view that LMXB spin periods should be in the millisecond range. The present observations constrain the region of the observational parameter space in P_{pul}, dP_{pul}/dt, and pulse fraction A for which pulsations may be detectable in these sources.

As Table 2 shows, results cannot be expressed simply as upper limits on A. For each source the upper limit is a function of the pulse period both because of instrumental limitations (telemetry time resolution imposes a maximum frequency above which we cannot search) and because of the frequency dependence in the expressions given in § 3 for upper limits. In general the higher the frequency, the higher the modulation depth A that remains consistent with the present observations. It is also true that if the orbital period is shorter than 3 hr, then the limits in Table 2, except for those pertaining to 4U 1820−30, must be replaced with substantially higher number; that is, an orbital period $\ll 3$ hr is another way that a millisecond pulsar could have escaped detection in this search. In

TABLE 2

LIMITS ON PULSE FRACTION IN LOW-MASS X-RAY BINARIES[a]

Source	"Other" Name	A (50 Hz)	A (400 Hz)	A (1600 Hz)	Minimum P_{orb} (hr)
Sco X-1	X1617−155	0.0019	0.0026	...	[b]
GX 340+0...........	X1642−455	0.0069	0.014	...	3
GX 5−1	X1758−250	0.0039	0.0077	...	3
		0.0031	0.0042	...	6
GX 9+1	X1758−205	0.0057	0.011	...	3
GX 17+2	X1813−140	0.0055	0.011	...	3
4U 1820−30	X1820−303	0.006	...	...	[c]
Cyg X-3	X2030+407	0.012	0.040	0.065	[d]
Cyg X-2	X2142+380	0.0051	0.010	...	[e]

[a] Modulation depth upper limit at 95% confidence level.
[b] Known period (19.2 hr).
[c] Known period (685 s).
[d] Known period (4.8 hr).
[e] Known period ($9^d.8$).

a source with an unknown orbital period, such as GX $5-1$, one must conclude that either the pulse period is within the searched range but the pulsed fraction is below 0.004, or that the pulsed period is shorter than 2 ms, or that the orbital period is substantially shorter than 3 hr, or a combination of these possibilities.

In the absence of a detected periodicity the indirect methods described in § 2 remain the best information on LMXB spin periods. Shorter pulse periods are both harder to detect, as reflected in the variation of upper limits with frequency, and easier to obliterate with scattering. Thus, our results may be characterized as being consistent with low pulse amplitudes and very short pulse periods in these objects, but they provide only weak support because there remain ways to hide a longer period. The importance of knowing the spin periods directly will undoubtedly motivate further searches.

These limits are lower than most of those in the earlier published literature because of the large collecting areas involved and the utilization of CRT. It may be useful to summarize ways that future searches can reach still lower limits. First, using higher telemetry resolution, even with the same detector area, allows one to achieve lower limits on A, even at the frequencies that have been searched here. Higher time resolution will also give further access to shorter periods, especially those below 2 ms where the present data are limited to the *HEAO 1* observation of Cyg X-3. Second, additional computer power will make it possible to use CRT on longer data segments. The maximum segment length N that can be searched grows roughly as the one-third power of CPU time or linearly with available RAM. Note however that integration time must not become a large fraction of the orbital period. Third, it must be recognized that the only way to reach *much* lower levels of modulation is with larger collecting area. An increase by a factor of 100 would be desirable.

The authors wish to express their thanks to F. Makino and the *Ginga* team for the excellent hospitality they have enjoyed during numerous visits to ISAS. This collaboration was made possible by grants from the National Aeronautics and Space Administration to NRL and Stanford. K. S. W., J. P. N., and P. H. acknowledge partial support for this work from the Office of Naval Research. W. H. G. L. acknowledges support from NASA under grants NAG 8-571, NAG 8-674, and NSG-7643. M. v d K. acknowledges support from the Leids Kerkhoven Bosscha Fund.

APPENDIX A

COHERENCE RECOVERY IN THE FREQUENCY DOMAIN

Instead of rebinning the data in the time domain, the analysis can be implemented in the frequency domain by means of an optimal linear filter. This filter has an especially simple form if the noise spectral density is independent of frequency (i.e., white noise). The optimal filter $M^*(\omega)$ is the Fourier transform of a specified function, $S(t)$, a trial source signal modified by orbital modulation. $M^*(\omega)$ depends on the trial signal frequency ω, and the quadratic parameter α, both of which are unknown; hence a two-dimensional grid of trial values must be searched. If α is zero, the problem reduces to computing the power spectrum of the input data. In the following, $S(t)$ is assumed to be real. $M^*(\omega)$ is approximated by its discrete Fourier transform and is the complex conjugate of the Fourier transform of the trial source function,

$$M^*(\omega_n) = \sum_{j=1}^{N} S(t_j) \exp(-2\pi ijn/N) . \tag{A1}$$

The time t_j is $j\tau$, where τ has been chosen to have unit value by convention. The parameter n is an index for the value of ω and runs from 0 to $N/2$. For a source function which is linear in frequency, quadratic in phase, $S(t)$ is of the form

$$S(t_j) = A \cos [\omega_s(t_j + \alpha t_j^2) + \phi] . \tag{A2}$$

This expression embodies the quadratic time transformation of equation (2). Substituting $S(t_j)$ in equation (A1) and letting $t_0 = T_{\rm int}/2$, we can write

$$M(\omega_n, \omega_s, m) = \frac{A}{2} e^{i\phi} \sum_j \exp\left[\left(\frac{n+s+msj}{N^2}\right)\frac{2\pi ij}{N}\right] + \frac{A}{2} e^{-i\phi} \sum_j \exp\left[\left(\frac{n-s-msj}{N^2}\right)\frac{2\pi ij}{N}\right], \tag{A3}$$

where s is an index for ω_s in analogy with n.

The output obtained when the filter is applied to the input data in the frequency domain is given by

$$F_f(\omega_s, m) = \sum_n F(\omega_n) M^*(\omega_n, \omega_s, m) , \tag{A4}$$

where $F(\omega_n)$ is the FFT of the input data and $m = \alpha\tau N^2$. The range of m is therefore $\pm N_\alpha/2$. For $m = 0$, $F_f(\omega_s, 0) = F(\omega_s)$, provided that M is properly normalized, and the FFT of the original data is recovered.

Notice that the expression for M^* in equation (A3) consists of two sums. Since n and s are both restricted to the range $[0, N-1]$, the first sum will always be small compared to the second sum. The second sum peaks near $n = s + ms/N$ and has a width about this value of order $\Delta n = 2ms/N$. Thus we will ignore the first sum and approximate the filter function by

$$M(\omega_n, \omega_s, m) = \frac{A}{2} \sum_j \exp\left[\left(\frac{n-s-msj}{N^2}\right)\frac{2\pi ij}{N}\right]. \tag{A5}$$

The phase factor $e^{-i\phi}$ has been dropped since the power spectrum is unaffected by the choice of phase:

$$P(\omega_s, m) = \left| \sum N(\omega_n) M^*(\omega_n, \omega_s, m) \right|^2 . \tag{A6}$$

In principle, M must be computed for all possible values of s and m. An efficient way to do this is to directly compute the FFT of the source function given by equation (A5) for each value of m. Then the power spectrum defined in equation (A6) can be computed. In general the right-hand side of this equation requires $2N$ multiplications and N additions for each value of m. However, because the filter function M^* is strongly peaked over a narrow frequency range, the computation of the power spectrum in practice depends on m and s, requiring of order $4ms/N \ll N$ multiplications and additions. The essential number of operations vanishes as s (i.e., frequency) approaches zero; this reflects the fact that for CRT performed in the time domain, the set of quadratic transformations results in identical power spectra near the DC channel and (completely) independent spectral channels only near the Nyquist frequency. For s corresponding to $\nu_{\rm Nyq}$, the number of multiplies required is $\sim 2N_\alpha$.

An additional computational savings is achieved by recognizing that equation (A5) implies the scaling rule

$$M(\omega_n, \omega_{s+\Delta s}, m) = M[\omega_{n-\Delta s}, \omega_s, m(1 + \Delta s/s)] . \tag{A7}$$

If a particular value of s is chosen, say $N/4$ (the center frequency bin of the FFT), then M can be computed for any other value of s from the above scaling relation.

The computational cost of constructing the filter array scales as $N_\alpha N \log_2(N)$; that is, the cost is roughly the same as performing CRT in the time domain for N_α quadratic time transformations and FFTs. However, since application of the filter requires a small number of operations (and the FFT of the input data is computed only once), a large savings results if several segments of input data are processed with identical CRT parameters and therefore make use of the same filter array.

APPENDIX B

LOSS OF POWER DUE TO FINITE GRID EFFECTS

We now consider the loss of power due to mismatch between the optimum value of α and the nearest value in the sequence of α values. Consider a purely sinusoidal signal. Ignoring the effects of finite binning, the signal is described by $r_j = r_0 \sin(\omega_{\rm pul} t_j)$, in the absence of any orbital motion. Here $t_j = j\tau$, where τ is the finite time bin size. We make the approximation that the signal is completely recovered for the optimum α value. If the optimum value of α differs from the nearest value in the sequence by an amount $\Delta\alpha$, the observed signal, to lowest order in $\Delta\alpha$, will be

$$r_j = r_0 \sin[\omega_{\rm pul}(t_j + \Delta\alpha t_j^2)] = r_0 \sin(\omega_{\rm pul} j\tau + \omega_{\rm pul}\Delta\alpha j^2\tau^2) . \tag{B1}$$

The power, $P(\omega_{\rm pul})$, is then

$$P(\omega_{\rm pul}) = \frac{1}{N_\gamma}\left[\sum_{j=1}^{N} r_0 \sin(\omega_{\rm pul} j\tau + \omega_{\rm pul}\Delta\alpha j^2\tau^2) e^{i\omega_{\rm pul} j\tau}\right]^2 . \tag{B2}$$

Rewriting the sum as an integral and separating the sine and cosine contributions, we obtain

$$P(\omega_{\rm pul}) = \frac{r_0^2}{N_\gamma}\left\{\int_0^{T_{\rm int}} [\sin(\omega_{\rm pul} t + \omega_{\rm pul}\Delta\alpha t^2)\cos(\omega_{\rm pul} t) + i \sin(\omega_{\rm pul} t + \omega_{\rm pul}\Delta\alpha t^2)\sin(\omega_{\rm pul} t)]dt\right\}^2 . \tag{B3}$$

Expanding the sine and ignoring the rapidly oscillating odd terms yields

$$P(\omega_{\rm pul}) \simeq \frac{r_0^2}{N_\gamma}\left\{\int_0^{T_{\rm int}} [\cos^2(\omega_{\rm pul} t)\sin(\omega_{\rm pul}\Delta\alpha t^2) + i \sin^2(\omega_{\rm pul} t)\cos(\omega_{\rm pul}\Delta\alpha t^2)]dt\right\}^2 . \tag{B4}$$

Because $\Delta\alpha t \ll 1$ (typically $\Delta\alpha \sim 10^{-9}\ {\rm s}^{-1}$ and $T_{\rm int} \sim 10^3$ s), the $\sin(\omega_{\rm pul}\Delta\alpha t^2)$ and $\cos(\omega_{\rm pul}\Delta\alpha t^2)$ terms are envelopes for the rapidly oscillating even terms $\cos^2(\omega_{\rm pul} t)$ and $\sin^2(\omega_{\rm pul} t)$, respectively. We can thus replace the $\sin^2(\omega_{\rm pul} t)$ and $\cos^2(\omega_{\rm pul} t)$ terms with their averages, namely $\frac{1}{2}$. We are left with

$$P(\omega_{\rm pul}) \simeq \frac{r_0^2}{4N_\gamma}\left\{\left[\int_0^{T_{\rm int}} \sin(\omega_{\rm pul}\Delta\alpha t^2)dt\right]^2 + \left[\int_0^{T_{\rm int}} \cos(\omega_{\rm pul}\Delta\alpha t^2)dt\right]^2\right\} . \tag{B5}$$

These can be rewritten as Fresnel integrals (e.g., § 7.3 of Abramowitz & Stegun 1968),

$$C(z) = \int_0^z \cos\left(\frac{\pi}{2} t^2\right)dt , \qquad S(z) = \int_0^z \sin\left(\frac{\pi}{2} t^2\right)dt . \tag{B6}$$

With appropriate substitutions we have

$$P(\omega_{\rm pul}) \simeq \frac{r_0^2 T_{\rm int}^2}{4N_\gamma}\left[\frac{C^2(x) + S^2(x)}{x^2}\right] , \tag{B7}$$

where $x = T_{\rm int}(2\omega_{\rm pul}\Delta\alpha/\pi)^{1/2}$.

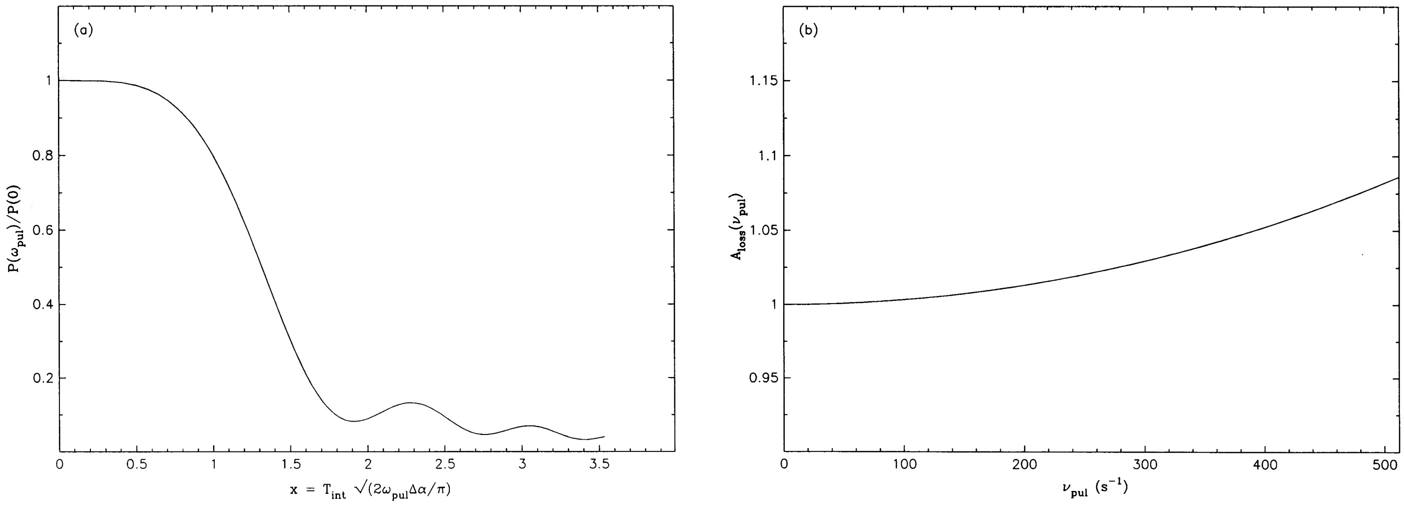

FIG. 3.—(*a*) Power recovered from quadratic transformations (CRT) as a function of quadratic parameter mismatch. Power is normalized to unity at zero frequency and is plotted as a function of scaled frequency x. (*b*) Loss of pulse amplitude due to quadratic parameter mismatch as a function of pulse frequency for the *Ginga* pulsar searches described in § 4.

In Figure 3*a* we plot $P(x)$ normalized to unity at zero frequency, that is, $P(x)/P(0)$ where x is given above. The pulse amplitude correction factor $A_{\rm loss}(\omega_{\rm pul})$ is defined to be

$$A_{\rm loss}(\omega_{\rm pul}) = \frac{1}{\sqrt{P(\omega_{\rm pul})/P(0)}} \simeq \left[\frac{C^2(x) + s^2(x)}{x^2}\right]^{-1/2} . \tag{B8}$$

Figure 3*b* shows $A_{\rm loss}$ as a function of signal frequency $\nu_{\rm pul} = \omega_{\rm pul}/2\pi$. To obtain $A_{\rm loss}$ we fix $\nu_{\rm pul}$ and average over $\Delta\alpha$ from $-\delta\alpha/2$ to $+\delta\alpha/2$, where $\delta\alpha = P_{\rm Nyq}/(2T_{\rm int}^2)$, the value used in our searches. Note that as in the case of finite binning, the effect becomes more pronounced at higher frequencies. The loss of power is $1/A_{\rm loss}(\omega_{\rm pul})^2$.

REFERENCES

Abramowitz, M., & Stegun, I. 1968, Handbook of Mathematical Functions (Washington: National Bureau of Standards)
Alpar, M. A., & Shaham, J. 1985, Nature, 316, 239
Angelini, L., Stella, L., & Parmar, A. N. 1989, ApJ, 346, 906
Bhattcharya, D. 1989, in Proc. 23rd ESLAB Symp.: Two Topics in X-ray Astronomy, ed. J. Hunt & B. Battrick (Noordwijk: ESA), 1, 179
Bhattacharya, D., & van den Heuvel, E. P. J. 1990, Phys. Rep., in press
Brainerd, J., & Lamb, F. K. 1987, ApJ, 317, L33
Bussard, R. W., Weisskopf, M. C., Elsner, R. F., & Shibazaki, N. 1988, ApJ, 327, 284
Chandrasekhar, S. 1970, Phys. Rev. Letters, 24, 611
Cominsky, L., Jernigan, J. G., Ossmann, W., Doty, J., van Paradijs, J., & Lewin, W. H. G. 1980, ApJ, 242, 1102
Cominsky, L. R., & Wood, K. S. 1989, ApJ, 337, 485
Córdova, F. A., Garmire, G. P., & Lewin, W. H. G. L. 1979, Nature, 278, 529
Davies, S. R., Coe, M. J., & Wood, K. S. 1989, in Proc. 23rd ESLAB Symp.: Two Topics in X-ray Astronomy, ed. J. Hunt & B. Battrick (Noordwijk: ESA), 1, 381
Davies, S. R., Wood, K. S., & Coe, M. J. 1990, MNRAS, 245, 268
Friedman, J. L., Ipser, J. R., & Parker, L. 1986, ApJ, 304, 115
Friedman, J. L., & Schutz, B. F. 1978, ApJ, 222, 281
Ghosh, P., & Lamb, F. K. 1979a, ApJ, 232, 259
———. 1979b, ApJ, 235, 296
Grindlay, J. E., & Bailyn, C. D. 1988, Nature, 336, 48
Hasinger, G., Priedhorsky, W. C., & Middleditch, J. 1989, ApJ, 337, 843
Hasinger, G., & van der Klis, M. 1987, IAU Circ., No. 4489
———. 1989, A&A, 225, 79
Helfand, D. J., Ruderman, M. A., & Shaham, J. 1983, Nature, 304, 423
Hertz, P. 1990, Computers in Physics, 4, No. 1, 86
Hertz, P., Norris, J. P., Wood, K. S., Vaughan, B. A., & Michelson, P. F. 1990, ApJ, 354, 267
Joss, P. 1978, ApJ, 225, L123
Joss, P. C., & Rappaport, S. A. 1983, Nature, 304, 419
Kelley, R. L., Christian, D. J., Schoelkopf, R. J., & Swank, J. H. 1989, in Proc. 23rd ESLAP Symp.: Two Topics in X-ray Astronomy, ed. J. Hunt & B. Battrick (Noordwijk: ESA) 1, 459
Kluźniak, W., & Wilson, J. 1987, in Proc. 13th Texas Symp. on Relativistic Astrophysics, ed. M. P. Ulmer (Chicago: World Scientific)
Kulkarni, S. R. 1986, ApJ, 306, L85
Kulkarni, S. R., Narayan, R., & Romani, R. W. 1990, ApJ, 356, 174
Lamb, F. K. 1989, in Proc. 23rd ESLAB Symp.: Two Topics in X-ray Astronomy, ed. J. Hunt & B. Battrick (Noordwijk: ESA), 1, 215
Lamb, F. K., Shibazaki, N., Shaham, J., & Alpar, M. A. 1985, Nature, 317, 681
Leahy, D. A. 1987, IAU Circ., No. 4485
Leahy, D. A., Darbro, W., Elsner, R. F., Weisskopf, M. C., Sutherland, P. G., Kahn, S., & Grindlay, J. E. 1983, ApJ, 266, 160
Lewin, W. H. G., & Joss, P. C. 1983, in Accretion-driven Stellar X-ray Sources, ed. W. H. G. Lewin & E. P. J. van den Heuvel (Cambridge: Cambridge University Press), 41
Lewin, W. H. G., van Paradijs, J., & van der Klis, M. 1988, Space Sci. Rev., 46, 273
Makino, F. 1987, Ap. Letters Comm., 25, 223
Mason, K. O., Middleditch, J., Nelson, J. E., & White, N. E. 1980, Nature, 287, 516
Meekins, J. F., Wood, K. S., Hedler, R. L., Byram, E. T., Yentis, D. J., Chubb, T. A., & Friedman, H. 1984, ApJ, 278, 268
Mereghetti, S., & Grindlay, J. E. 1987, ApJ, 312, 727
Mészáros, P., Riffert, H., & Berthiaume, G. 1988, ApJ, 325, 204
Michelson, P. F., & Wood, K. S. 1989, MNRAS, 241, 769
Middleditch, J., & Priedhorsky, W. 1986, ApJ, 306, 230
Mitsuda, K., Dotani, T., Yoshida, A., Vaughan, B. A., & Norris, J. P. 1990, Pub. Astr. Soc. Japan, submitted
Murakami, T., Inoue, H., Makishima, K., & Hoshi, R. 1987, Pub. Astr. Soc. Japan, 39, 879
Norris, J. P., Hertz, P., Wood, K. S., Michelson, P. F., Vaughan, B. A., Mitsuda, K., & Dotani, T. 1990, ApJ, 361, 514
Norris, J. P., & Wood, K. S. 1987, ApJ, 312, 732
Paczynski, B. 1983, Nature, 304, 421
Parmar, A. N., & White, N. E. 1988, Mem. Soc. Astr. Italiana, 59, 147
Parmar, A. N., White, N. E., Giommi, P., & Gottwald, M. 1986, ApJ, 308, 199
Parsignault, D., & Grindlay, J. E. 1978, ApJ, 225, 970
Rappaport, S. 1989, talk presented at 23rd ESLAB Symp.: Two Topics in X-ray Astronomy, 1989 September 13–20, Bologna, Italy
Robinson, E. L. 1983, in Cataclysmic Variables and Related Objects, ed. M. Livio & G. Shaviv (Dordrecht: Reidel), 1
Romani, R. W. 1990, Nature, 347, 741
Ruderman, M. 1990, ApJ, submitted
Sadeh, D., Byram, E. T., Chubb, T. A., Friedman, H. F., Hedler, R. L., Meekins, J. F., Wood, K. S., & Yentis, D. J. 1982, ApJ, 257, 214
Savonije, G. J. 1983, Nature, 304, 422

Shakura, N. I., & Sunyaev, R. A. 1973, A&A, 24, 337
Shibazaki, N. 1989, in Proc. 23rd ESLAB Symp.: Two Topics in X-ray Astronomy, ed. J. Hunt & B. Battrick (Noordwijk: ESA), 1, 237
Shibazaki, N., Murakami, T., Shaham, J., & Nomoto, K. 1989, Nature, 342, 656
Stella, L., White, N. E., & Priedhorsky, W. 1987, ApJ, 315, L49
Taam, R. E., & van den Heuvel, E. P. J. 1986, ApJ, 305, 235
Tawara, Y., Hayakawa, S., Kunieda, H., Makino, F., & Nagase, F. 1982, Nature, 299, 38
Turner, M. J. L., et al. 1989, Pub. Astr. Soc. Japan, 41, 345
van den Heuvel, E., van Paradijs, J., & Taam, R. E. 1986, Nature, 322, 153
van der Klis, M. 1989, ARA&A, 27, 517
van der Klis, M., Jansen, F., van Paradijs, J., Lewin, W. H. G., van den Heuvel, E. P. J., Trümper, J. E., & Sztajno, M. 1985, Nature, 316, 225
van Paradijs, J., Hasinger, G., Lewin, W. H. G., van der Klis, M., Sztajno, M., Schulz, N., & Jansen, F. 1988, MNRAS, 231, 379
Verbunt, F., Lewin, W. H. G., & van Paradijs, J. 1989, MNRAS, 241, 51
Verbunt, F., Wijers, R. A. M. J., & Burm, H. M. G. 1990, A&A, 234, 195
Wagoner, R. V. 1984, ApJ, 278, 345
Wang, Y.-M., & Schlickeiser, R. 1987, ApJ, 313, 200
Wood, K. S., Ftaclas, C., & Kearney, M. 1988, ApJ, 324, L63
Wood, K. S., Hertz, P., Norris, J. P., Vaughan, B. A., Michelson, P. F., Mitsuda, K., & Dotani, T. 1989, in Proc. 23rd ESLAB Symp.: Two Topics in X-ray Astronomy, ed. J. Hunt & B. Battrick (Noordwijk: ESA), 1, 689
Wood, K. S., et al. 1984, ApJS, 56, 507
Wood, K. S., Norris, J. P., Hertz, P., & Michelson, P. F. 1987, in Variability of Galactic and Extragalactic X-ray Sources, ed. A. Treves (Milan: Associazione per l'Avancement dell'Astronomia), 213